

An Evolutionary Method for Kinetic Energy Ammunition Optimization

Alexandre A. Motta, Nelson F. F. Ebecken

NTT/COPPE/Universidade Federal do Rio de Janeiro
Cidade Universitária, CT Bloco B Sala 100
Caixa Postal: 68506
Rio de Janeiro, RJ, Brazil - 21945-970

Abstract

A research is being carried on to optimise long rod penetrators used in kinetic energy munitions. Kinetic energy munitions performance can be measured by the penetration achieved in a normal impact on a semi-infinite steel plate (rolled homogeneous armour, RHA). For a reference target (fixed characteristics and distance) performance will depend of the properties and characteristics of the penetrator and the propellant charge, assuming that no changes will be made in the firing gun. The properties and characteristics of the propellant charge and of the penetrator will dictate the terminal velocity and how the penetrator will interact with the target. This is a well known problem with several proved models available in the literature. However, no method has been proposed to find an optimal configuration. In the present work, the penetration achieved with a particular configuration (set of parameters) is combined with relevant penalizations thus providing its fitness for ranking by the Genetic Algorithm code in the search for an optimal configuration.

Keywords: Kinetic Energy Ammunition, Long Rod Penetrator, Optimization, Genetic Algorithms, Impact

I. INTRODUCTION

“Long rod penetrators are modern equivalents of the cannonball, intended to pierce a target by depositing large amounts of kinetic energy in a concentrated region” (Wright, 1983).

Kinetic energy (*KE*) ammunition is mainly used to attack armour. The long rod penetrator is the option of choice to defeat heavy tanks by tanks. The theory for the one-dimensional penetration of semi-finite targets by long rods is based in the work from Tate (1967, 1969) and Alekseevskii (1966). It describes the interaction between the penetrator and the target and attempts to predict the characteristics of the resulting crater in the last. The literature in this subject is vast and many authors have provided valuable contributions to it, like the overviews made by Zook et al. (1992), Goldsmith (1999) and Orphal (2006), the survey carried on by Wright (1983) and the database produced by Anderson et al. (1992). Other authors have also carried on analytical, numerical and experimental studies and proposed extensions or modifications to the Alekseevskii-Tate model, like Rosenberg (1990), Jones et al. (1987), Wang and Jones (1996), Grace (1993), Walker et al. (1995), Rubin and Yarin (2002), Walters (1991), Seglets and Walters (2003), Walker (2001), Lan and Wen (2010) and Wen et al. (2010, 2011).

The strike velocity determines the regime at which the interaction between long rods and rolled homogenous armour (*RHA*). Penetration is governed by plastic deformation mechanism for strike

velocities up to 1,150m/s (Bennett, 1998 and Longdon, 1987) and hydrodynamic behaviour occurs at strike velocities greater than several km/s, like in shaped charge munitions (Doig, 1998). Typical strike velocities for long rod munitions are in the range between 1,500m/s and 1,700m/s and both mechanisms are observed (Bennett, 1998). Designers seek to achieve the maximum possible strike velocity upon impact, combined with long penetrators made of materials with higher density than the expected target. This is supported by experimental work (Hohler & Stilp, 1997 and 1978).

Bennett (1998), however, points out that although “first thoughts suggest that continual improvements in penetration by means of higher strike velocities with ever longer and more dense penetrators might be relatively easy to achieve”, “more careful thought shows that these features interact with each other, and with other important factors such as the internal and external ballistics, the forces on both the ammunition and the gun, and the ammunition stowage and handling”. The author describes the consequences of increasing the long rod length, keeping all other parameters constant. Among others, an increased surface area will increase the drag and reduce the strike velocity, a longer, heavier sabot will be required for in-bore stability (with greater parasite mass) and an increased higher peak pressure, due to the higher inertia of the heavier shot, will be observed resulting in higher stresses in the barrel, not to mention the reduction in muzzle

velocity.

The models for interior, exterior and terminal ballistics of long rods presented by Bennett (1998) were selected for use in the present work to estimate the performance achieved using configurations described by a set of parameters. These models are summarized in sections 2.1, 2.2 and 2.3. For consistency, the parameters herein are limited to: penetrator diameter, penetrator length-diameter ratio, penetrator density, sabot-penetrator length ratio, sabot mean diameter-bore diameter ratio, sabot density, charge mass, charge force constant, charge α , charge β , charge ballistic size, charge form function and propellant shape. Gun chamber volume and shot travel were not considered because they are related to the gun, not the ammunition. Each set of parameters (variables) constitutes an individual in the Genetic Algorithm (GA) application. Fitness is measured by the penetration achieved in a target (RHA) positioned 1,000m away from the muzzle.

The machine used in the present development until the submission of the present article was a "domestic" PC (processor Intel(R) Core(TM) i5-2500K, 4GB RAM, Windows 7 Professional). All implementation was carried on using Fortran.

II. BALLISTIC MODELS

2.1 Interior Ballistics Model

Bennett (1998) proposed the use of the lumped parameter model as presented in Longdon (1987). The behaviour of the gas during the combustion and its expansion processes are described in terms of the average gas properties and rates of change. According to the author, this assumption is particularly adequate near the muzzle and therefore suitable to predict the muzzle velocity and the peak pressure. This model calculates the muzzle velocity, allowing the determination of the shot trajectory and the strike velocity. All names and subscripts used by Bennett (1998) were kept for consistency.

Piobert's law governs the combustion of the propellant and it is assumed that all surfaces burn inwards at a constant burn rate. The ballistic grain size D is measured as the shortest distance between opposing sides and combustion ends when these sides meet and D equals zero. The burning rate depends on the ambient pressure and is defined by the fraction f of D remaining at a time t :

$$\frac{df}{dt} = - \frac{\beta p^\alpha}{D}, \quad (1)$$

where α (the burning rate coefficient) and β (the burning rate index) depend on the propellant.

The geometry of the propellant grain determines the relationship between f and the mass fraction of burnt propellant (z) through a semi-empirical

constant, the form function (c):

$$z = (1 - f)(1 + cf). \quad (2)$$

The energy released during combustion of the propellant charge can be evaluated according to:

$$E_p = E_s + E_g + E_u + E_r + E_q + E_\epsilon + E_\mu \quad (3)$$

where:

E_p = energy released by the propellant charge

E_s = shot KE

E_g = gas KE

E_u = unburnt propellant KE

E_r = recoiling mass (gun) KE

E_q = gas residual heat

E_ϵ = barrel strain energy

E_μ = shot friction

Typically, the strain energy of the gun is less than 0.5 % of the total energy and can be neglected (Longdon, 1987). The equations of motion for the shot travelling inside the barrel can be written as:

$$m \frac{dv}{dt} = A_b (P_s - P_a) - R_f \quad (4)$$

$$v = \frac{dx}{dt}$$

where:

m = combined mass of the penetrator and the sabot

v = shot velocity

x = shot displacement in the barrel

A_b = bore cross-section

P_s = shot base pressure

P_a = atmospheric pressure

R_f = resistance to motion (friction)

Fourth order Runge-Kutta integration was used to calculate the muzzle velocity, the maximum chamber pressure and the shot motion, allowing the determination of the maximum nominal sabot shear stress (NSSS – the first constraint in this application), the maximum value achieved by the breech pressure (the second constraint, assumed to be equal to P_b) and the all-burnt position (AB, the last constraint). The AB is the position in the bore the projectile is in the instant that all propellant charge is burned.

2.2. Exterior Ballistics Model

For long rod penetrators, the distance between leaving the gun and striking the target is generally no more than 3,000m and therefore the trajectory lasts 2s or less hence, the only factors that need to be

considered are drag and gravity (Bennett, 1998). This model allows the determination of the strike velocity, required to determine the penetration in the target.

The drag force (F_D) can be calculated as:

$$F_D = F_N + F_S + F_B + F_X + F_F \quad (5)$$

where:

- F_N = nose drag
- F_S = skin drag
- F_B = base drag
- F_X = excrescence drag
- F_F = fin drag

Drag forces are calculated using Eq. 6 (McCoy, 1999):

$$F = \frac{1}{2} \rho C_D \left(\frac{\pi d^2}{4} \right) v^2, \quad (6)$$

where:

- C_D = drag coefficient
- d = penetrator diameter
- v = penetrator velocity
- ρ = air density

And the equations of motion for the projectile become:

$$\begin{aligned} m_p \ddot{x}_1 &= - F_D \cos(\theta) \\ m_p \ddot{x}_2 &= - F_D \sin(\theta) - m_p g \end{aligned} \quad (7)$$

where:

- m_p = penetrator mass
- x_1 = horizontal displacement from the muzzle
- x_2 = vertical displacement from the muzzle
- θ = angle between the penetrator velocity vector and the horizontal

2.3. Terminal Ballistics Model

Finally, the model adopted by Bennett (1998) starts assuming hydrodynamic penetration, similarly to the model presented by Held (1991) for shaped charges.

After the initial contact, the velocity of the rear of the penetrator is assumed to be constant, equal to

the strike velocity, v . As the penetration process develops, the crater growth is assumed to happen at a constant rate, u . Using Bernoulli, it is possible to write:

$$\rho_p (v - u)^2 = \rho_t u^2, \quad (8)$$

where:

- ρ_p = penetrator density
- ρ_t = target density
- v = strike velocity
- u = crater growth rate

It is also assumed that the crater stops growing when the whole penetrator is eroded. Therefore:

$$\frac{L}{v - u} = \frac{P}{u}, \quad (9)$$

where:

- L = penetrator length
- P = penetration depth

Rearranging Eq. 8 and 9, the penetration equation can be obtained:

$$\frac{P}{L} = \sqrt{\frac{\rho_p}{\rho_t}}, \quad (10)$$

Since the strike velocity is below the lower limit for pure hydrodynamic penetration, an experimentally determined coefficient, k , is added to Eq. 10:

$$\frac{P}{L} = k \sqrt{\frac{\rho_p}{\rho_t}}, \quad (11)$$

Bennett (1998) proceeds providing a sample set of data (presented in section 2.4) which was adopted as reference.

2.4. Data and Limits

The data used by Bennett (1998) was used as approximate central values for the minimum and maximum values for each variable of the problem. These values and the lower and upper limits for each variable are presented in Table 1.

Table 1: Data and limits for the variables and constraints in the application

Variable	Bennett (1998)	Minimum	Maximum
penetrator diameter	0.025 m	0.020 m	0.030 m
penetrator length-diameter ratio	16.0	12.0	20.0
penetrator density	16,500 kg/m ³	14,000 kg/m ³	18,600 kg/m ³
sabot-penetrator length ratio	0.760	0.500	0.850
sabot mean diam-bore diam ratio	0.500	0.500	0.850
sabot density	2,710 kg/m ³	2,000 kg/m ³	7,850 kg/m ³
charge mass	6.700 kg	6.500 kg	7.200 kg
charge force constant	951,000 J/kg	940,000 J/kg	1,050,000 J/kg
charge α	1.680E-9	1.680E-9	1.680E-9
charge β	0.993	0.950	1.000
charge ballistic size	0.0015 m	0.0012 m	0.0018 m
charge form function	0.190	-0.050	0.200
propellant shape	stick	Stick	
Constraint			
N_{SSS}	63 MPa	N/A	100 MPa
P_b	462 MPa	N/A	550 MPa
AB	33%	27%	35%

III. METHOD AND INITIAL RESULTS

3.1 The method

The choice for *GA* as optimization method follows from the problem characteristics: it is a multi-variable problem with conflicting objectives and a variety of constraints. The implementation was validated using the examples provided in Bennett (1998).

In *GA*, a random population is generated and a value of fitness is attributed to each individual. Individuals in a given population are ranked according to this value and elitism, cross-over and mutation operations can be applied producing a new generation. This generation will be ranked as the first and new operations may be applied (Goldberg, 1989 and Motta, 2004). This is repeated successively until a criterion is met – in the present work a previously selected number of generations.

The strategy used by Motta & Ebecken (2006) was selected for the present work: each set of parameters (or variables) were arranged in an array, constituting an individual, a set of individuals constituting a generation. The main difference is that binary codification was only used to perform cross-over and mutation operations. All other operations were performed in decimal, double precision codification. Similarly to this work, random mono-point cross-over and mutation operations were implemented in non-elite members of the population.

An initial population of individuals with random attributes (valid variable values) is generated and their fitness determined, after which they are ranked and the non-elite members submitted to cross-over and mutation operations (according to the respective probabilities of occurrence), resulting in a new generation. This process is repeated until a criterion is reached (in this work, a pre-selected number of

generations).

The process to determine the fitness of an individual – or a configuration, a set of variables, followed the ballistic model described in item 2: the muzzle velocity was calculated using the interior ballistics model, feeding the exterior ballistics model to determine the strike velocity which was used by the terminal ballistics model to determine the penetration achieved by that configuration.

The constraints AB , N_{SSS} and P_b calculated in the interior ballistics model and other characteristics such as penetrator length or charge mass can be used to penalize a configuration. Initially, individuals with values outside the limits shown in Table 1 were given nil fitness but this strategy proved to lead to results that although reasonably similar and improved when compared to state-of-art ammunition performance lacked convergence in a strict sense. Therefore, other penalisation methods are being tested as discussed in item 3.2.

3.2 Sensitivity

A sensitivity analyses was conducted to provide insight with respect to the impact of small variations in the values of the variables on performance. Charge mass variation was selected to illustrate this in the present work. Simulations were run with fixed values for all variables but the charge mass (all in the valid range) as shown in Table 2. The results are presented in Table 3. The application returned zero fitness for some values but it was not continue. It can be observed that variations in the charge mass between 7.01043 kg and 7.01473 kg – only 430 g, produce and unexpected result. The non-zero values in Table 3 are plotted in Fig. 1. These results are reproducible.

This model is highly sensitive to small variations in the parameters and this impacts convergence, as

shown in item 3.3.

Table 2: Parameters for sensitiveness analysis

Variable	Value	Minimum	Maximum
penetrator diameter	0.02870 m	0.020 m	0.030 m
penetrator length-diameter ratio	19.75	12.0	20.0
penetrator density	18202 kg/m ³	14000 kg/m ³	18600 kg/m ³
sabot-penetrator length ratio	0.600	0.500	0.850
sabot mean diam-bore diam ratio	0.540	0.500	0.850
sabot density	2137.64 kg/m ³	2000 kg/m ³	7850 kg/m ³
charge mass	variable	6.500 kg	7.200 kg
charge force constant	1032460 J/kg	940000 J/kg	1050000 J/kg
charge α	1.6760E-09	1.680E-9	1.680E-9
charge β	0.995	0.950	1.000
charge ballistic size	1.70 E-3 m	1.20E-3 m	1.8E-3 m
charge form function	0.095	-0.050	0.200
propellant shape	stick	stick or grain	
gun chamber volume	0.0078 m	0.007 m ³	0.009 m ³
shot travel	6.611 m	4.50 m	7.20 m

Table 3: Fitness according to the variation of the charge mass

Charge Mass (kg)	Penetration (m)
7.01043	0.66063
7.01065	0.66068
7.01086	0.66073
7.01108	0.00000
7.01129	0.00000
7.01151	0.00000
7.01172	0.00000
7.01194	0.00000
7.01215	0.00000
7.01237	0.00000
7.01258	0.66114
7.01280	0.66074
7.01301	0.66079
7.01323	0.66084
7.01344	0.66089
7.01366	0.66095
7.01387	0.66100
7.01409	0.66105
7.01430	0.66110
7.01452	0.00000
7.01473	0.66120

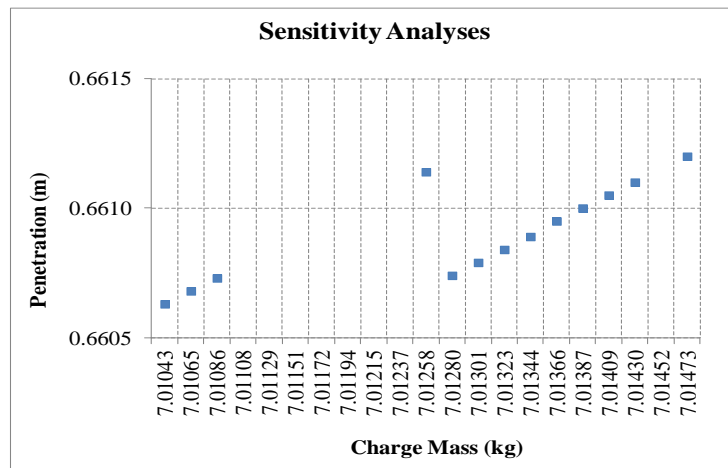


Fig. 1: Sensitivity analyses: fitness variation according to different charge masses

3.3 Convergence

In this work, convergence refers to the generation in which the best fit individual (the set of parameters that resulted in the highest penetration) was found. After the implementation strategy was resolved, it was decided to use a population with 400 individuals – it was not observed a direct correlation between the size of the population and convergence although populations with less than 100 individuals

were not tried. The rates of elitism, cross-over and mutation also seemed to have little impact in convergence.

Table 4 shows five results obtained after 10,000 generations with 2% elitism, 70% cross-over rate and 90% mutation rate. One may argue that these rates are exaggerated, but virtually dozen executions with varied rates showed no direct correlation between them and convergence or the results obtained.

Table 4: Results obtained after 10,000 generations

Elitism	2%				
Cross-over rate	70%				
Mutation Rate	90%				
Generations	10000				
Execution #:	1	2	3	4	5
Highest Fitness:	0.5177	0.5111	0.5076	0.5163	0.5205
Generation:	7268	5555	2053	6777	8384
Best fit indiv.:					
Penetrator Diam	0.0203	0.0223	0.0228	0.0218	0.0223
Pen L-D Ratio	18.9196	19.6382	19.0821	19.3108	19.3809
Penetrator Dens	17748.150	15705.612	15541.733	16458.950	17455.637
Sabot L-Ratio	0.6587	0.5909	0.5527	0.6233	0.6341
Sabot Diam-Ratio	0.5328	0.5615	0.5251	0.5357	0.5079
Sabot Density	2349.428	2048.758	2324.745	2039.092	2115.995
Charge Mass	7.1599	6.8416	7.0982	6.9152	7.1960
Charge Force Constant	1.050E+06	1.045E+06	1.040E+06	1.025E+06	1.026E+06
Charge α	0.9983	0.9965	0.9910	0.9977	0.9969
Charge β	1.718E-09	1.567E-09	1.786E-09	1.794E-09	1.541E-09
Charge Ball. Size	0.0016	0.0014	0.0014	0.0015	0.0014
Charge Form Func	0.1015	0.1241	-0.0451	0.0254	-0.0456
Constraints:					
AB	0.3214	0.3113	0.3045	0.2702	0.3165
$NSSS$	1.736E+07	1.693E+07	1.878E+07	1.666E+07	1.750E+07
P_b	1.158E+08	1.086E+08	1.142E+08	1.074E+08	1.142E+08

Convergence for the executions showed in Table 4 can be observed in Fig. 2. The results are very good and above what is expected in practical terms for this

type of ammunition, but it is not considered that convergence was achieved. It should be noted that a logarithmic scale was used for the Generation axis

(horizontal). Table 5 and Fig. 3 show the same outputs for 30,000 generations without any improvement in the convergence. Table 6 and Fig. 4 present the results using different cross-over rates and Table 7 and Fig. 5 present the results using different mutation rates (10,000 generations).

There are noticeable differences in the values of most variables and clearly the method, as is, did not achieve what is expected, a unique, reproducible solution. Increasing the number of generations did not produce any impact in the convergence.

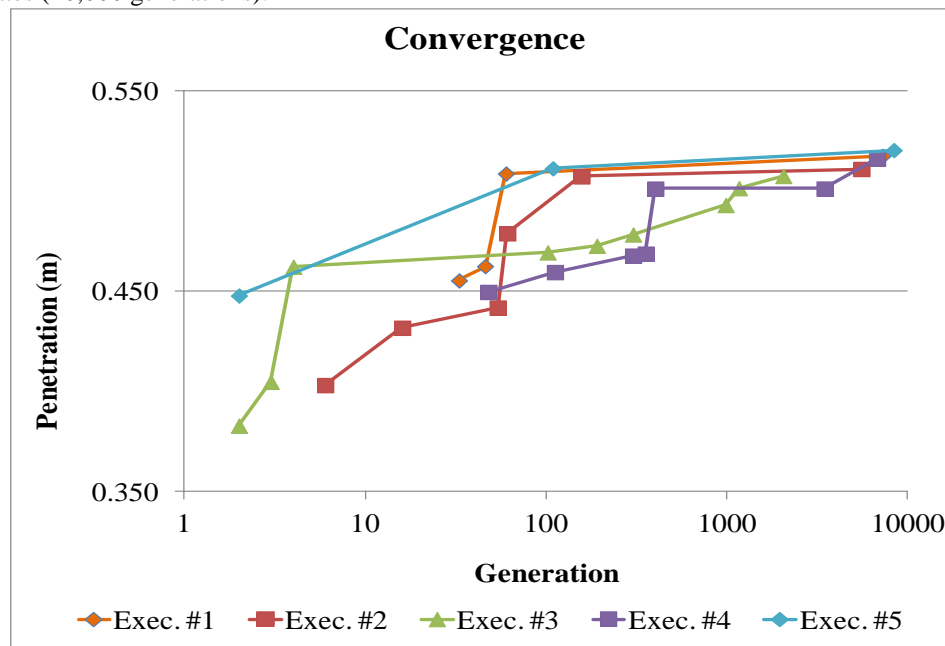


Fig. 2: Convergence (penetration achieved) after 10,000 generations

Table 5: Results obtained after 30,000 generations

Elitism	2%				
Cross-over rate	70%				
Mutation Rate	90%				
Generations	30000				
Execution #:	1	2	3	4	5
Highest Fitness:	0.5187	0.5206	0.5117	0.5206	0.5180
Generation:	14959	7666	26695	28076	22069
Best fit indiv.:					
Penetrator Diam	0.0222	0.0212	0.0204	0.0225	0.0212
Pen L-D Ratio	19.9960	19.7749	19.8852	19.6862	19.3110
Penetrator Dens	14852.957	17817.392	16355.482	16325.378	17694.685
Sabot L-Ratio	0.5688	0.6081	0.6338	0.7042	0.6546
Sabot Diam-Ratio	0.5550	0.5020	0.5679	0.5173	0.5079
Sabot Density	2210.531	2361.125	2197.778	2017.631	2055.335
Charge Mass	7.0600	7.1561	7.1919	7.1252	6.6124
Charge Force Const	1.045E+06	1.007E+06	1.042E+06	1.048E+06	1.047E+06
Charge α	0.9989	0.9928	0.9956	0.9830	0.9924
Charge β	1.772E-09	1.548E-09	1.561E-09	1.698E-09	1.558E-09
Charge Ball. Size	0.0017	0.0013	0.0014	0.0013	0.0012
Charge Form Funct	0.0567	0.0845	-0.0038	0.1582	0.1427
Constraints:					
<i>AB</i>	0.3041	0.3401	0.3452	0.3473	0.2946
<i>NSSS</i>	1.713E+07	1.799E+07	1.698E+07	1.460E+07	1.676E+07
<i>P_b</i>	1.130E+08	1.110E+08	1.182E+08	1.135E+08	1.050E+08

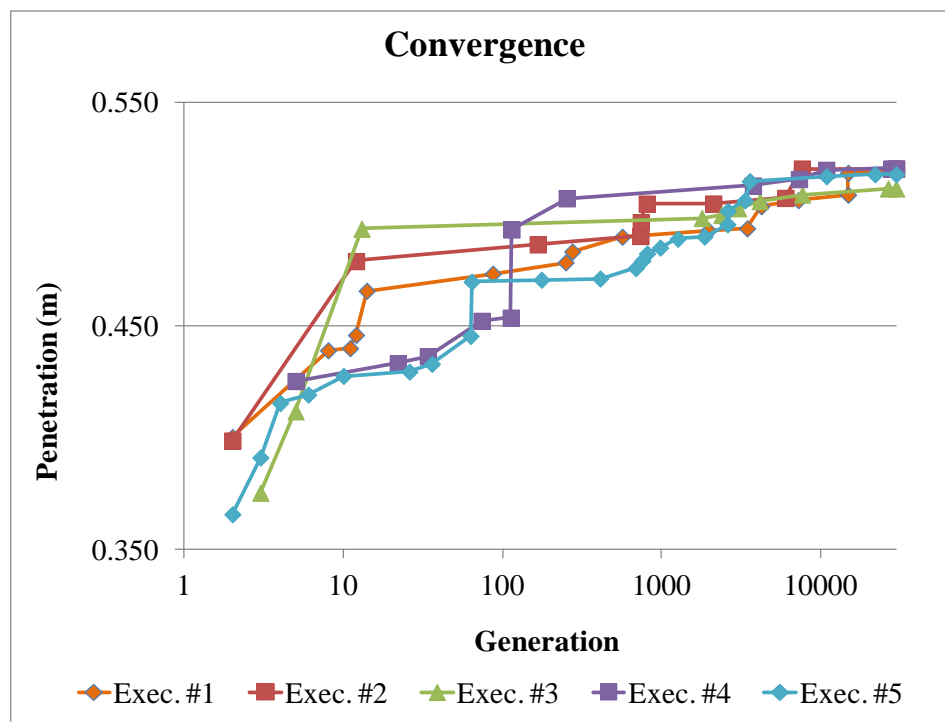


Fig. 3: Convergence (penetration achieved) after 30,000 generations

Table 6: Results obtained after 10,000 generations using different cross-over rates

Execution #:	1	2	3	4	5
Elitism	2%				
Cross-over rate	40%	50%	60%	70%	80%
Mutation Rate	90%				
Generations	10000				
Highest Fitness:	0.5211	0.5209	0.5195	0.5060	0.5116
Generation:	1774	7195	6288	7707	3770
Best fit indiv.:					
Penetrator Diam	0.0205	0.0229	0.0224	0.0202	0.0212
Pen L-D Ratio	19.3443	19.9995	19.9028	19.9048	19.1149
Penetrator Dens	17858.288	14360.685	15729.378	17897.276	17923.025
Sabot L-Ratio	0.6459	0.5269	0.5638	0.7234	0.6661
Sabot Diam-Ratio	0.5309	0.5370	0.6065	0.5759	0.5218
Sabot Density	2212.802	2232.409	2068.758	2158.166	2117.647
Charge Mass	7.1469	7.0328	7.1450	6.9197	7.0469
Charge Force Const	1.014E+06	1.044E+06	1.043E+06	1.047E+06	1.037E+06
Charge α	0.9923	0.9853	0.9849	0.9851	0.9940
Charge β	1.686E-09	1.724E-09	1.720E-09	1.781E-09	1.629E-09
Charge Ball. Size	0.0014	0.0012	0.0013	0.0013	0.0014
Charge Form Funct	0.1509	0.0520	0.0174	0.1493	0.0258
Constraints:					
AB	0.3441	0.3179	0.3096	0.3161	0.3441
NSSS	17241404	18332357	17828085	14438789	17242462
P_b	111372340	112782270	113922250	109518160	113924370

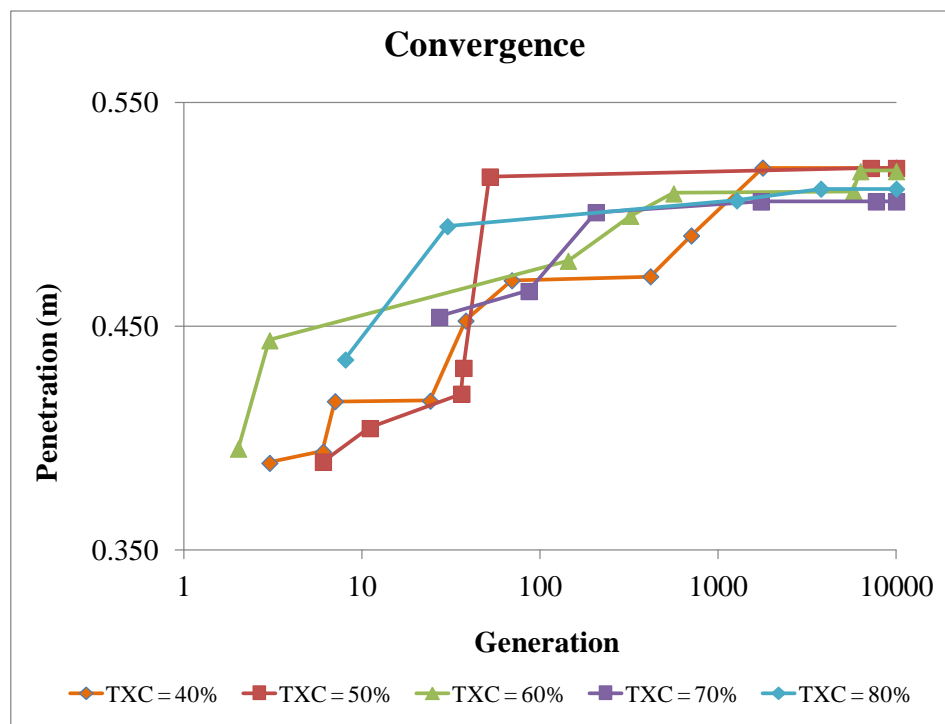


Fig. 4: Convergence after 10,000 generations using different cross-over rates

Table 7: Results obtained after 10,000 generations using different mutation rates

Execution #:	1	2	3	4	5
Elitism	2%				
Cross-over rate	50%				
Mutation Rate	40%	50%	60%	70%	80%
Generations	10000				
Highest Fitness:	0.5276	0.5151	0.5193	0.5277	0.5252
Generation:	3392	5747	8601	9743	7733
Best fit indiv.:					
Penetrator Diam	0.0215	0.0208	0.0204	0.0206	0.0214
Pen L-D Ratio	19.8844	19.0818	19.0538	19.5370	19.9750
Penetrator Dens	16431.377	17454.163	18282.739	17792.577	17078.896
Sabot L-Ratio	0.6682	0.6437	0.6325	0.6188	0.5974
Sabot Diam-Ratio	0.5378	0.5110	0.5115	0.5309	0.5317
Sabot Density	2009.819	2267.297	2405.675	2271.450	2166.429
Charge Mass	7.0769	6.8986	7.0421	7.1705	7.0330
Charge Force Const	1.040E+06	1.022E+06	1.034E+06	1.025E+06	1.020E+06
Charge α	0.9954	0.9896	0.9993	0.9951	0.9863
Charge β	1.748E-09	1.677E-09	1.610E-09	1.550E-09	1.695E-09
Charge Ball. Size	0.0016	0.0012	0.0014	0.0013	0.0013
Charge Form Funct	0.1812	0.1128	0.0062	0.0401	0.1252
Constraints:					
AB	0.3466	0.2813	0.2945	0.3211	0.3424
NSSS	15651065	16730535	18227144	18199768	17863689
P_b	112576340	106645640	112342570	113637770	110342740

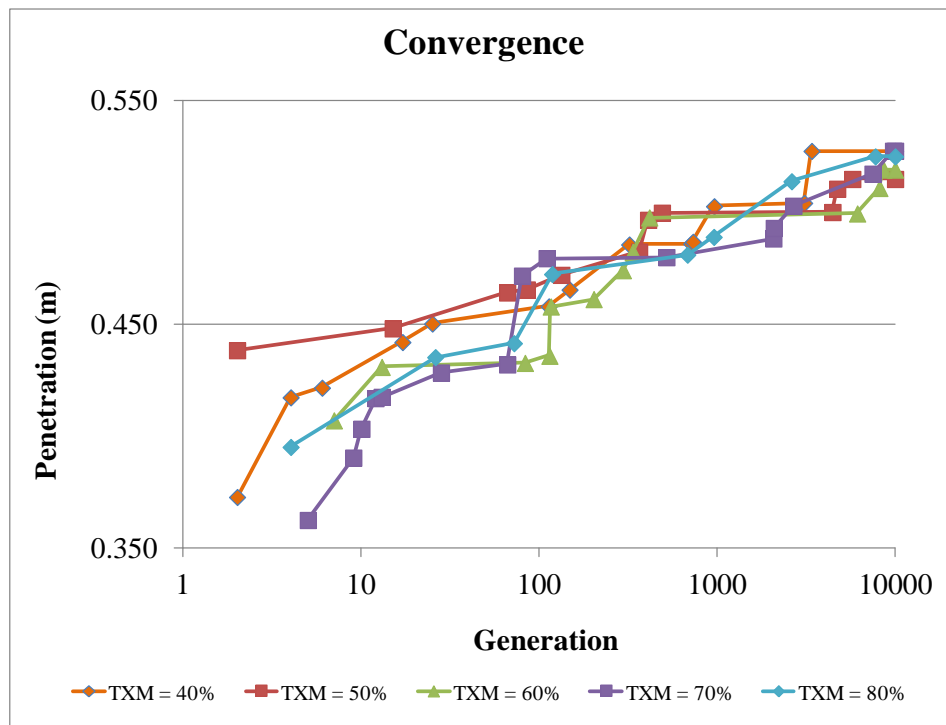


Fig. 5: Convergence after 10,000 generations using different mutation rates

3.4 Other strategies to improve convergence

In order to improve convergence, different penalisation strategies promoting smoother, gradual reduction on fitness as the variables approach the limits of the allowed intervals are implemented. Such strategies were used by Motta & Ebecken (2006) and account for less tangible aspects like loss of accuracy as *AB* moves away from the centre of the allowed interval, increased stowage space required for longer rounds, cost etc. Figure 6 shows multipliers that can

be used to penalise the individuals according to the constraints. The curve for *AB* is parametric of fourth order and was designed to not heavily penalise central values (with respect to the allowed range). The other curves represent linear progressive penalisation after a threshold is reached. These implemented penalisations are for demonstration purposes and specific rules must be developed for individual cases.

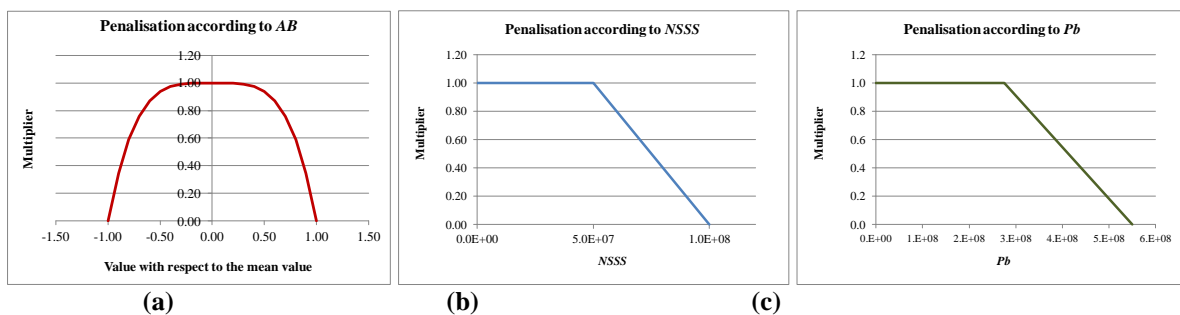


Fig. 6: Penalisations for *AB* (a), *NSSS* (b) and *Pb* (c)

Table 8 and Fig. 7 show the results and convergence evolution applying such constraint-related penalties. It can be observed that this conservative approach leads to lower penetration values and that the most fit individual may not be the one with highest penetration.

Table 8: Results obtained using constraint-related penalisation

Execution #:	1	2	3	4	5
Elitism	2%				
Cross-over rate	70%				
Mutation Rate	90%				
Generations	10000				
Highest Fitness:	0.3665	0.3696	0.3788	0.3729	0.3757
Highest Penetration:	0.3920	0.3829	0.3868	0.3797	0.3873
Generation:	7687	3392	6174	391	4712
Best fit indiv.:					
Penetrator Diam	0.0201	0.0208	0.0202	0.0201	0.0204
Pen L-D Ratio	19.9345	19.0921	19.8904	18.6665	19.9337
Penetrator Dens	17698.183	18069.224	18251.671	15333.106	17402.227
Sabot L-Ratio	0.8213	0.7625	0.7575	0.7652	0.7173
Sabot Diam-Ratio	0.5101	0.5049	0.5016	0.5051	0.5103
Sabot Density	2146.130	2089.920	2286.510	2091.233	2198.692
Charge Mass	7.1219	7.1595	7.1907	7.1768	7.1778
Charge Force Const	9.923E+05	1.007E+06	1.033E+06	1.032E+06	1.038E+06
Charge α	0.9733	0.9819	0.9888	0.9903	0.9887
Charge β	1.783E-09	1.693E-09	1.525E-09	1.732E-09	1.737E-09
Charge Ball. Size	0.0013	0.0014	0.0015	0.0016	0.0017
Charge Form Funct	0.1221	0.0153	-0.0158	-0.0359	0.0116

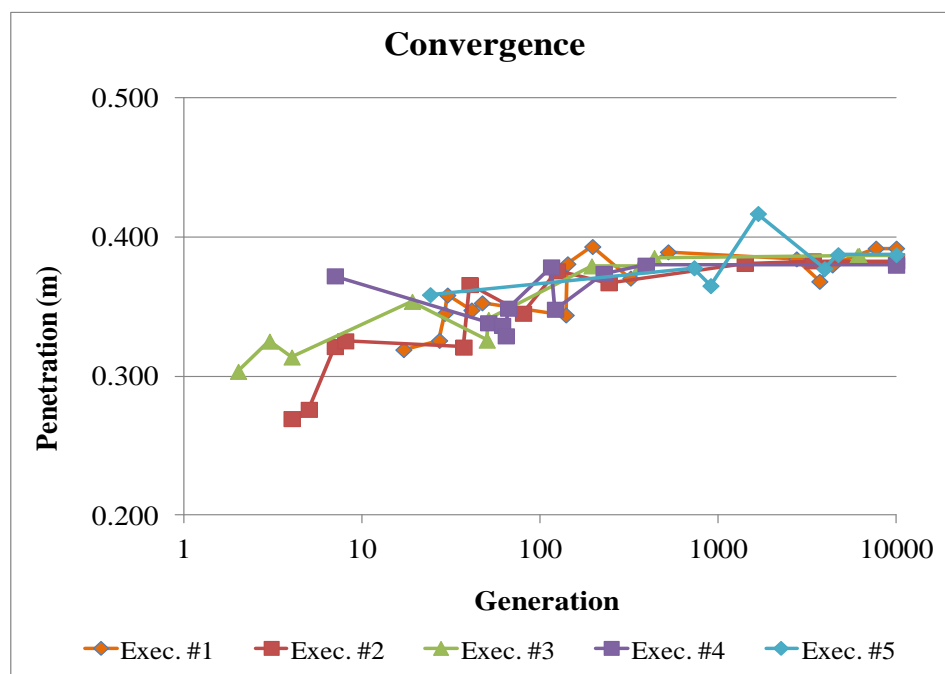


Fig. 7: Convergence applying constraint-related penalties

Analysts should pay attention to the fact that the individual with higher penetration (performance) may not be the best fit in the population and thoughtful considerations might be necessary to assess whether adequate penalisation criteria are in place.

IV. CONCLUSION

The problem of finding an optimal kinetic ammunition (long rod only) using evolutionary methods is a challenging task due to the high

sensitivity of the problem to small variations in the variables involved. The present work is based on the model proposed by Bennett (1998). As the author cites in his work, 'the results show clearly the interdependence between the various gun and ammunition parameters, and the penetration that can be achieved'.

The method herein proposed allowed to identify physically meaningful sets of parameters that result in very high penetrations, of the order of 50% above

the highest value presented in Bennett (1998). Despite of the lack of convergence to a single value – meaning that improvements are still required to find ‘the optimal’ set of parameters, the method provides means to investigate the interdependence between the variables. The resulting differences do not disqualify the method but reinforce the need for keeping a critical thinking.

Traditionally, ammunition designers rely on empirical data and experience to conceive new munitions. The present method provides a novel, innovative approach to improve performance, intending to determine the optimal parameters in the configuration of kinetic ammunition (long rod only). The method can also be easily modified to adopt other models or to take into consideration other set of variables.

V. SUMMARY

The present work introduces a method for the optimization of kinetic energy (long rod only) ammunition with respect to its terminal effects on steel homogeneous targets using an evolutionary method, i.e. Genetic Algorithms. The terminal effect, its performance, is measured by the penetration achieved against rolled homogenous armour (steel) at a fixed distance.

The model adopted in the present work is simple, yet accurate enough to produce acceptable results, including all relevant aspects of the physical problem. It can be altered and improved, but increasing the complexity of the calculations does not alter the purpose of the method presented. Therefore, a simpler model is preferable for demonstration purposes.

Although convergence of the method is yet to be understood and modifications must be implemented to allow the identification of the optimal configuration, results already provide valuable insights on the study of this class of problems and can be used to suggest design modifications to improve performance.

Finally, the authors suggest that artificial intelligence / machine learning can also be incorporated with potential improved results, as well as more sophisticated models.

REFERENCES

- [1.] Alekseevskii, V. P., 1966. Penetration of a Rod into a Target at High Velocity, Combustion, Explosion and Shock Waves; 2: 63-66.
- [2.] Anderson Jr, C. E., Morris, B. L. & Littlefield, D. L., 1992. A Penetration Mechanics Database. SwRI Report 3593/001, Southwest Research Institute, San Antonio, TX.
- [3.] Bennett, M. D., 1998. Long Rod Penetration Performance, *Journal of Battlefield Technology*, Vol. 1, No. 3, pp. 1-6.
- [4.] Doig, A., 1998. Some Metallurgical Aspects of Shaped Charge Liners, *Journal of Battlefield Technology*, Vol. 1, No. 1, pp. 1-3.
- [5.] Goldberg, D. E., 1989. Genetic Algorithms in Search, Optimization, and Machine Learning. Addison-Wesley: Boston., MA, USA.
- [6.] Goldsmith, W., 1999. Non-Ideal Projectile Impact on Targets, *International Journal of Impact Engineering*; 22: 95-395.
- [7.] Grace, F. I., 1993. Nonsteady Penetration of Long Rods into Semi-Infinite Targets, *International Journal of Impact Engineering*; 14: 303-314.
- [8.] Held, M., 1991. Hydrodynamic Theory of Shaped Charge Jet Penetration, *Journal of Explosives and Propellants*, Vol. 9, pp. 9-24.
- [9.] Hohler, V. & Stilp, A., 1977. Penetration of Steel and High Density Rods in Semi-Infinite Steel Targets, *Proceedings Third International Symposium on Ballistics*, Karlsruhe, Germany.
- [10.] Hohler, V. & Stilp, A., 1978. Study of the Penetration Behaviour of Rods for a Wide Range of Target Densities", *Proceedings Fourth International Symposium on Ballistics*, Monterey, California.
- [11.] Lan, B., & Wen, H. M., 2010. Alekseevskii-Tate Revisited: an Extension to the Modified Hydrodynamic Theory of Long-Rod Penetration, *Sci. China, Ser. E*. 53(5): 1364-1373.
- [12.] Longdon, L.W., 1987. Textbook of Gunnery and Ballistics, Vol. 1, HMSO, London.
- [13.] McCoy, R. L., 1999. Modern Exterior Ballistics, Schiffer Publishing Ltd, Atglen, PA.
- [14.] Motta, A. A., 2004. Underwater Explosive Charges Optimization with Respect to Their Terminal Effects on Submerged Steel Structures. DSc Dissertation, Federal University of Rio de Janeiro/Rio de Janeiro.
- [15.] Motta, A.A., & Ebecken, N.F.F, 2006. On the Application of Genetic Algorithms in Underwater Explosive Charges Optimization, *International Journal for Computational Methods in Engineering Science and Mechanics*, Vol. 8, Iss. 1. DOI: 10.1080/15502280601006140.
- [16.] Jones, S. E., Gillis, P. P. & Foster, J. C., 1987. On the penetration of semi-infinite targets by long Rods. *Journal of the Mechanics and Physics of Solids*; 35(1): 121-131.

- [17.] Orphal, D. L., 2006. Explosions and Impacts, *International Journal of Impact Engineering*; 33: 496-545.
- [18.] Rosenberg, Z., 1990. On the Hydrodynamic Theory of Long-Rod Penetration, *International Journal of Impact Engineering*; 10: 483-486.
- [19.] Rubin, M. B. & Yarin, A. L., 2002. A Generalized Formula for the Penetration Depth of a Deformable Projectile, *International Journal of Impact Engineering*; 27: 387-398.
- [20.] Segletes, S. B. & Walters, W. P., 2003. Extensions to the Exact Solution of the Long Rod Penetration/Erosion Equations, *International Journal of Impact Engineering*; 28: 363-376.
- [21.] Tate, A., 1967. A Theory for the Deceleration of Long Rods after Impact, *Journal of the Mechanics and Physics of Solids*; 15: 387-399.
- [22.] Tate, A., 1969. Further Results in the Theory of Long Rod Penetration, *Journal of the Mechanics and Physics of Solids*, 17, 141-15C.
- [23.] Walker, J. D. & Anderson Jr, C. E., 1995. A Time-Dependent Model for Long-Rod Penetration, *International Journal of Impact Engineering*; 16(1): 19-48.
- [24.] Walker, J. D., 2001. Hypervelocity Penetration Modeling: Momentum VS. Energy and Energy Transfer Mechanisms, *International Journal of Impact Engineering*; 26: 809-822.
- [25.] Walters, W. P. & Segletes, S. B., 1991. An Exact Solution of the Long Rod Penetration Equations, *International Journal of Impact Engineering*; 11(2): 225-231.
- [26.] Wang, P. & Jones, S. E., 1996. An Elementary Theory of One-Dimensional Rod Penetration Using a New Estimate for Pressure, *International Journal of Impact Engineering*; 18(3): 265-279.
- [27.] Wen, H.M., He, Y. & Lan, B., 2011. A combined numerical and theoretical study on the penetration of a jacketed Rod into semi-infinite target. *International Journal of Impact Engineering*; 38:1001-1010.
- [28.] Wen, H.M., He, Y. & Lan, B., 2010. Analytical Model for Cratering of Semi-Infinite Metal Targets by Long Rod Penetration, *Sci. China, Tech. Sci.*; 53: 3189-3196.
- [29.] Wright, T. W., 1983. A Survey of Penetration Mechanics for Long Rods, In J. Chandra and J. E. Flaherty (eds.), *Computational Aspects of Penetration Mechanics*, Springer, New York, pp. 85-106.
- [30.] Zook, J. A., Frank, K. & Silsby, G. F., 1992. Terminal Ballistics Test and Analysis Guidelines for the Penetration Branch, BRL-MR-3960, U.S. Army Ballistic Research Laboratory, Aberdeen Proving Ground, MD.